

Deep Learning Based Spatial User Mapping on Extra Large MIMO Arrays

Abolfazl Amiri, Carles Navarro Manchón, Elisabeth de Carvalho

Department of Electronic Systems, Aalborg University, Denmark
Email: {aba,cnm,edc}@es.aau.dk

Abstract—In an extra-large scale MIMO (XL-MIMO) system, the antenna arrays have a large physical size that goes beyond the dimensions in traditional MIMO systems. Because of this large dimensionality, the optimization of an XL-MIMO system leads to solutions with prohibitive complexity when relying on conventional optimization tools. In this paper we propose a design based on machine learning for the downlink of a multi-user setting with linear pre-processing, where the goal is to select a limited *mapping area* per user, i.e. a small portion of the array that contains the beamforming energy to the user. We refer to this selection as *spatial user mapping* (SUM). Our solution relies on learning using deep convolutional neural networks with a distributed architecture that is built to manage the large system dimension. This architecture contains one network per user where all the networks work in parallel and exploit specific non-stationary properties of the channels along the array. Our results show that, once the parallel networks are trained, they provide the optimal SUM solution in more than 80% of the instances, resulting in a negligible sum-rate loss compared to a system using the optimal SUM solution while providing an insightful approach to rethink these kinds of problems that have no closed-form solution.

I. INTRODUCTION

Massive multiple-input multiple-output (MIMO) antenna systems are one of the most promising solutions for fulfilling the demands for upcoming fifth generation (5G) wireless mobile communication systems [1]. While first pilots of 5G are being launched, there is a lot of attention among researchers for *beyond-5G* topics [2]. One of the most popular research avenues is that of extending the amount of antenna elements present in base stations (BS) beyond typical massive MIMO configurations, which has been referred to in the literature as *extra large scale MIMO array (XL-MIMO)* [3] or *large intelligent surfaces* [4].

One viable way to realize XL-MIMO systems is to use the infrastructure of large venues like airports, stadiums, etc. in order to place antenna elements. They can be deployed all in one location or distributed across a large area. Having enormous number of antennas provides extreme spatial resolution that can be used to boost throughput and spectral efficiency, support a larger number of users and extend the wireless service coverage area.

One of the main challenges faced for the successful application of XL-MIMO is the fact that, as the number of elements of the arrays—and consequently, the dimension of the XL-MIMO matrix—increases, so does the complexity of

the associated baseband processing for tasks such as MIMO precoding and detection. There is thus a need to design efficient signal processing tools that deal with large-dimensional problems and are scalable [5]. In this context, machine learning (ML) and, in particular, deep learning methods emerge as an almost indispensable tool to revisit complex scenarios. Deep neural networks (DNNs) and especially convolutional neural networks (CNNs) have achieved considerable success in countless applications [6], [7]. Recently, they have attracted lots of attention in the field of wireless communications. Different problems in the physical layer such as rate maximization, modulation schemes, power control are investigated using machine learning techniques [8].

In this work, we explore the application of DNNs to the problem of spatial user mapping and MIMO precoding in the downlink of XL-MIMO systems. Motivated by the fact that different parts of the array may experience different propagation environments due to the large physical dimensions of XL-MIMO arrays, we pose a model for the XL-MIMO channel in which the signal received from (or transmitted to) a given user concentrates most of its energy over a limited portion of the array, which we call the visibility region (VR) of the user [9]. Under such conditions, we realize that most of the gain from the XL-MIMO system can be achieved by precoding the signals transmitted to a given user over just a subset of the array elements belonging to its VR, rather than the whole array. Our goal is then to find the optimal subset of antennas for each user, given a fixed zero-forcing (ZF) precoder design and under a constraint on the maximum number of antennas that can be used for each of the users. Since solving the problem optimally requires combinatorial complexity, we instead train a deep CNN structure to perform the task. Once the network is trained, it provides a competitive solution for the user mapping problem in comparison to the current state-of-the-art, as shown in our simulation results, the trained CNN is able to produce the optimal solution with high success rate and with negligible loss in terms of average sum-rate with respect to optimal ZF precoding over all the array elements.

A. Related Works and Contribution

Several works have already explored the application of DNN's to problems arising in MIMO communications. For example, the authors of [10] use a deep learning framework

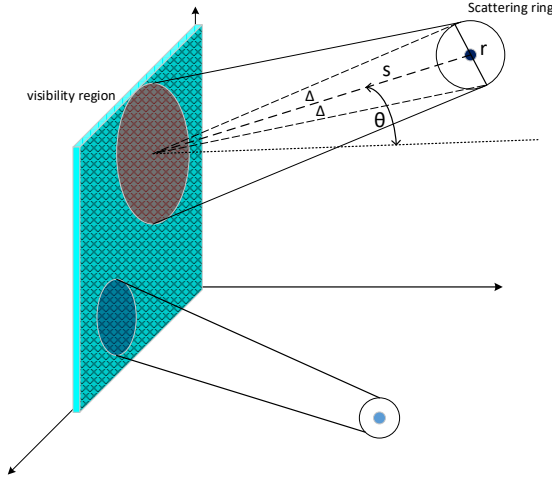


Fig. 1. An example of XL-MIMO array with spatial non-stationary regions along the array. Each user has a specific visibility region according to the channel conditions.

to solve problems such as signal to noise and interference ratio (SINR) balancing, power minimization and sum-rate maximization in a MISO downlink system with 6 antennas. An application of ML for selecting antenna sets in MIMO systems is presented in [11], where the authors use well-known ML tools in a small MIMO system with 8 antennas. The work in [12] focuses on antenna selection (AS) problem in a multi-antenna (20 antennas) system and constructs a CNN as a multi-class classification framework where each class designates a different subarray.

In all the aforementioned works, however, the system dimensions are limited and the effects of extra-large arrays are not explored. Contrary to this, we propose in this article a CNN based solution for the SUM problem in XL-MIMO arrays, where the signal received from (or transmitted to) a given user has most of its energy confined in the user's VR. Classical solutions to the AS problem such as [13] are not practical for XL-MIMO, as the complexity explodes due to the increased channel dimensions. In our design, we keep the computational complexity contained by exploiting the users' VRs to distribute the SUM problem into a set of identical CNN's that can be run in parallel for each of the users. The simulation results show that our proposed solution performs very closely to optimal ZF-precoding over the whole antenna array, avoiding the exhaustive search technique. To the best of our knowledge, this is the first work applying deep learning methods to XL-MIMO systems.

II. SYSTEM MODEL

Let M and K denote the number of antennas and simultaneously active users, respectively. We assume narrow-band transmissions; $\mathbf{x} \in \mathbb{C}^K$ denotes the vector of complex input symbols, $\mathbf{H} \in \mathbb{C}^{M \times K}$ is the complex channel matrix, $\mathbf{F} \in \mathbb{C}^{M \times K}$ is the MIMO precoding matrix and $n_k \sim \mathcal{CN}(0, \sigma_n^2)$

is the AWGN. We model the received baseband signal for user k with $y_k \in \mathbb{C}$ as follows:

$$y_k = \mathbf{h}_k^H \mathbf{F} \mathbf{x} + n_k. \quad (1)$$

where $(\cdot)^H$ shows conjugate transposition and \mathbf{h}_k denote the k -th column of \mathbf{H} , corresponding to user k . In this work, we adopt the following channel model [14]:

$$\mathbf{h}_k = \sqrt{w_k} \bar{\mathbf{h}}_k, \quad (2)$$

where w_k captures the effect of large scale fading which in turn is a function of the distance of the user from the array, denoted with s_k , and the propagation properties of the environment; here, we employ the following simplified propagation model [15]:

$$w_k = \beta_k s_k^\alpha, \quad (3)$$

where β_k is a attenuation coefficient [15] and α is the pathloss exponent. $\bar{\mathbf{h}}_k \sim \mathcal{CN}(0, \mathbf{R}_k)$ accounts for fast fading in a non-line of sight scenario, with \mathbf{R}_k being a symmetric positive semi-definite channel covariance matrix. We can represent channel vectors $\bar{\mathbf{h}}_k$ using Karhunen-Loeve expansion as

$$\bar{\mathbf{h}}_k = \mathbf{U}_k \mathbf{\Lambda}_k^{\frac{1}{2}} \mathbf{z}_k, \quad (4)$$

where $\mathbf{z}_k \in \mathbb{C}^{\zeta \times 1} \sim \mathcal{CN}(0, \mathbf{I})$, $\mathbf{\Lambda}_k$ is an $\zeta \times \zeta$ diagonal matrix with dominant eigenvalues and $\mathbf{U}_k \in \mathbb{C}^{M \times \zeta}$ is the tall unitary matrix of the eigenvectors of \mathbf{R}_k corresponding to the ζ dominant eigenvalues.

Using the well-known *one-ring* model [16] to define \mathbf{R}_k , the correlation between the channel coefficients of antennas p and q is given by

$$[\mathbf{R}_k]_{p,q} = \frac{1}{2\Delta} \int_{-\Delta}^{\Delta} \exp(j\mathbf{f}(\alpha + \theta)(\mathbf{u}_p - \mathbf{u}_q)) d\alpha, \quad (5)$$

where $\mathbf{f}(\nu) = -\frac{2\pi}{\lambda} (\cos(\nu), \sin(\nu))$ is the wave vector with angle of arrival of β , carrier wavelength of λ and $\mathbf{u}_p, \mathbf{u}_q \in \mathbb{R}^2$ are the position vectors of the antennas p, q within the VR of user k . Δ is angular spread which is $\Delta \approx \arctan(\frac{r}{s})$, with r standing for the ring of scatterers radius. Also, θ is the azimuth angle of user k with respect to antenna array (See Fig. 1). When either of the antenna indices p, q is outside the VR for user k , we have $[\mathbf{R}_k]_{p,q} = 0$. We use a uniform linear array (ULA) configuration and assume that the scattering rings are distributed uniformly in front of the array.

In this paper we consider the downlink (DL) data transmission and the target of SUM is to find the best antenna set for each of the users to send the signals. Due to the reciprocity of DL and uplink (UL) channels in time division duplex (TDD), each VR represents the region of the array that contains substantial portion of the user's energy, e.g. 95% of total received energy, in UL transmission. Therefore, one obvious consequence of having VR for each of the users is that the optimal SUM of each user should be inside its VR because the signal outside it is very weak and negligible. As it can be seen in Fig. 1, considering the antennas within VR of one user in the one-ring model results in dividing the array into binary regions. In order to model the distribution of the VRs we use a uniform distribution over the array for the VR

centers and a parametric uniform distribution for the length of VRs, i.e. $\text{VR}_{\text{length}} \sim U(l_1, l_2)$.

In order to formulate the precoder and the signal to noise and interference (SINR) of transmitting DL signal only on a subset of antennas or *processing window* for each user, we define \mathbf{H}_T as truncated channel. \mathbf{H}_T only contains the elements of \mathbf{H} on the processing window for each of the users. So, $\mathbf{H}_T = \mathbf{A} \odot \mathbf{H}$ where (\odot) stands for the element-wise matrix product and $\mathbf{A} \in \{0, 1\}^{M \times K}$ is a binary matrix with its (m, k) th element taking the value 1 if the m th antenna is within the processing window of the user k , and 0 otherwise. Thus, the truncated ZF beamformer is

$$\mathbf{F} = \sqrt{\frac{P_T}{\text{trace}(\mathbf{P}(\mathbf{H}_T^H \mathbf{H}_T)^{-1})}} \mathbf{H}_T (\mathbf{H}_T^H \mathbf{H}_T)^{-1} \quad (6)$$

where $\mathbf{P} = \text{diag}(P_{x_1}, P_{x_2}, \dots, P_{x_K})$ is a diagonal matrix with user signal powers, i.e. $P_{x_k} = \mathbb{E}\{x_k x_k^H\}$ and \mathbb{E} stands for expectation operator; P_T is the total transmit power. Finally the SINR for user k is equal to

$$\gamma_k = \frac{|\mathbf{h}_k^H \mathbf{f}_k|^2 P_{x_k}}{\sum_{k' \neq k} |\mathbf{h}_k^H \mathbf{f}_{k'}|^2 P_{x_{k'}} + \sigma_{n_k}^2}. \quad (7)$$

III. SPATIAL USER MAPPING PROBLEM FORMULATION

While the truncated ZF precoder in (6) does not guarantee interference free reception, as signals sent from antennas outside the mapping window of user k may still interfere user k 's reception, it has the advantage that the precoder for each user can be calculated based on a much smaller channel matrix: specifically, for computing user k 's precoder, one needs only to consider those columns of \mathbf{H}_T which contain non-zero elements within user k 's mapping window. Thus we expect that, if the mapping window of the users is chosen near-optimally, we obtain a noticeable complexity reduction at the expense of only a slight performance degradation with respect to the non-truncated ZF precoder.

To this end, we formulate the SUM problem as the selection of N_{max} antennas for each of the users that maximizes the system's sum-rate with the precoder (6), i.e.:

$$\max_{\{\mathbf{a}_k\}} \sum_{k=1}^K \log(1 + \gamma_k) \quad (8a)$$

$$\text{s.t. } \|\mathbf{a}_k\|_1 = N_{max}, \quad k = 1, 2, \dots, K \quad (8b)$$

where γ_k is the SINR for user k , \mathbf{a}_k is k th column of \mathbf{A} , $\|\mathbf{a}\|_1$ is the norm 1 of \mathbf{a} .

In general, solving (8) needs checking all the combinations of the antennas for all the users to see which one maximizes the sum-rate. The total number of the combinations is $K \frac{M!}{N_{max}!(M-N_{max})!}$ which is very large in our system. Therefore sub-optimal solutions were presented to use heuristic algorithms to locate best antenna sets to be selected [13]. On the other hand, the computational cost of these methods is huge and is impractical as M and K grow very large. Instead of solving the optimization directly, we propose in the next section a DNN structure which, once successfully trained, can

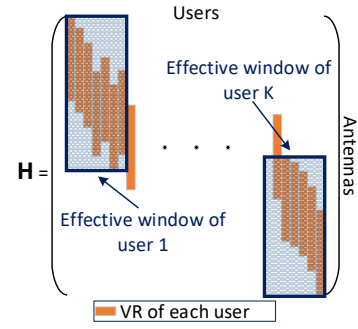


Fig. 2. An illustrative example of effective window concept. Only the interfering users affect one users signal and it is sufficient to consider only this part to extract the necessary information.

produce acceptable solutions while providing a useful way of rethinking the precoder design.

Having a XL-MIMO array provides a great spatial resolution to distinguish users signals better. For instance, users interference is limited to their VR overlaps and users with no VR intersection enjoy interference free environment. Since ZF solves a set of dependent linear equations by backward substitution algorithm, it treats independent equations as a new linear system and solves them separately. Thus, extending it to the concept of VR in XL-MIMO, recovering the signal within one VR is possible over the superposition of VRs of the interfering users (see Fig. 2). We call this subset of users and antennas *effective window*, and discuss its importance on the implementation of distributed CNNs in the next section.

IV. CNN DEEP LEARNING

As mentioned in the previous sections, the large dimensions of the problem prevents us from using simple learning methods such as K-nearest neighbors algorithm [11], which are impractical options for SUM in our context. As an alternative, convolutional neural networks have shown great performance in dealing with the problems in physical layer [8]. Especially when size of the optimization parameters is very large, there exist an appropriate CNN with enough depth and training data that can extract all the features perfectly. In this section we present our CNN's layer architecture and their goal.

A. Network Architecture

The dashed box in Fig. 3 shows the basic CNN design for the SUM problem. It consists of several layers starting with the input layer. To the best of our knowledge, current deep learning tools only work with real-valued data and therefore we enhance our original channel matrix data \mathbf{H} by adding other dimensions. Input data has a dimension of $M' \times K' \times 3$ where M' and K' are the antenna elements and the users present in the effective window, respectively. The third dimension contains the real, imaginary and phase of the entries.

Convolutional layers (CL) create several convolution kernels to be convolved with their input. These layers try to extract different features at each of their kernels and

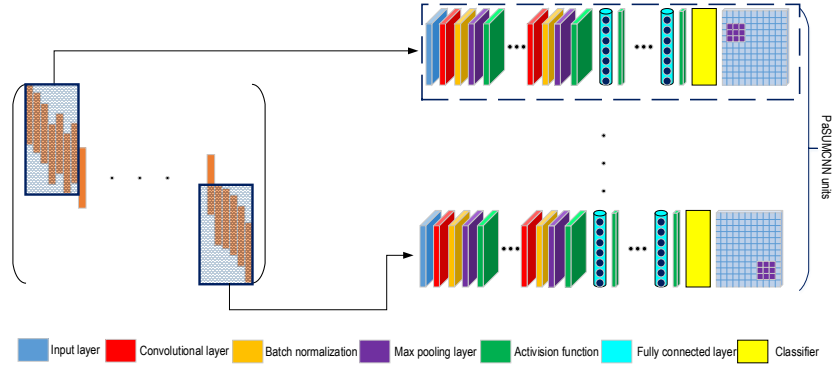


Fig. 3. Schematic of PaSUMCNN in distributed XL-MIMO. Each of these PaSUMCNN units are fed by the effective window of the corresponding user.

are vastly used for image processing applications. Similar to images, elements of the channel matrix \mathbf{H} have many similarities with their neighbor elements and we use this principle to implement two-dimensional CLs. Otherwise, one should put a *fully connected (FC) layer* with enormous number of neurons to capture this information. The latter solution is more complex due to its size and needs more training data.

Batch normalization (BN) layers are placed after each CL for normalization and scaling their input. They have two learnable parameters: *offset* and *factor* (See Table I). BNs help in avoiding over-fitting, accelerating convergence and reducing the sensitivity to the initialization of the weights [10]. Then, *Max pooling (MP)* layers are placed to reduce the dimension of BN's output by only keeping the maximum element within their specific pooling window.

Most importantly the nonlinear units known as activation functions (AF), which are the distinct difference between conventional linear systems, are used after MP and FC layers. Here, we use rectified linear units (ReLU) where the $\text{ReLU}(x) = \max(x, 0)$. FC layers are well-known hidden layers in the neural networks. Right before the output layer we put a *Flatten layer* which is a FC layer with number of the neurons equal to the number of the classes. This layer prepares the output for the *Soft-max layer* which calculates the probability distribution of the classes.

In order to optimize (8) using DNNs, similar to [12] we selected classification problem where each class stands for a set of N_{max} antennas indices with total number of \mathbb{C} classes. Since the VR for each of the users contains contiguous antenna elements over a region of the array and also to keep the complexity very low we assume these N_{max} antennas are adjacent. These \mathbb{C} classes are places in a uniform way to cover all the array elements. Then, we use the negative log-likelihood or cross-entropy loss function for the classifier. The accuracy of the classification is another metric that we use for evaluating the network's performance. We define accuracy as

$$\text{Accuracy}(\%) = \frac{T_s}{T} \times 100 \quad (9)$$

where T is the total number of samples in the training/evaluation datasets and T_s is the number of samples for which the classifier successfully selects the correct class.

B. Parallel CNNs

The most important obstacle for extending MIMO array size is the computational complexity growth. One way to deal with this burden is to employ distributed processing units [17]. One drawback of these methods compared to the central processing is to find the best solution to distribute tasks between the units. Inspired by the fact that sufficient information for detecting each user lies in its effective window region, we proposed parallel spatial user mapping convolutional neural networks (PaSUMCNN) for our problem. As shown in Fig. 3 each of these identical networks only processes the effective window of the desired user. This method has the following advantages:

- Small sized CNNs can be used since the size of the feature domain is limited.
- These small sized CNNs need ordinary distributed processing units that are not costly compared to ultra fast computing systems.
- All the units work in parallel and there is no extra delay for information exchanges between the units.

C. Spatial User Mapping Method for CNN Training

In this section we describe the training data design process and the main assumptions for the channel model and the training phase.

Algorithm 1 describes the training data generation procedure. After initializing with simulation and system parameters, it generates all the possible antenna selections for all the users in step 1. A set of N_{max} antenna indices is allocated for each user and users can have similar sets as well.

In the next step, a channel matrix is generated and is used for calculating SINR (7) and the sum-rate (8). Afterwards, the best configuration maximizing the sum-rate is selected as the solution for the SUM problem. The last step, concatenates the channel matrices and the labels for all of the samples. There is also one hidden step before feeding these training data to the CNNs and there we normalize and scale the channel matrices (same as BN layer) to avoid effects of using biased data. The normalization and scaling has the following form:

$$[\mathbf{H}]_{ij}^{\text{new}} = \frac{[\mathbf{H}]_{ij}^{\text{old}} - \frac{1}{M} \sum_i [\mathbf{H}]_{ij}^{\text{old}}}{\max_i [\mathbf{H}]_{ij}^{\text{old}} - \min_i [\mathbf{H}]_{ij}^{\text{old}}} \quad (10)$$

Algorithm 1 Training data generation.

Result: Labeled training and validation data for each of the PaSUMCNN units \mathcal{T}_k , $k = 1, \dots, K$

Initialize: M , K , N_{max} , \mathbb{C} , number of samples \mathbb{I} , σ_n^2 , \mathbf{P} , β , \mathbf{d} and α .

1. Calculate all possible antenna selection space \mathbf{Q} , where $|\mathbf{Q}| = K^{\mathbb{C}}$.

for $i = 1$ to \mathbb{I} **do**

2. Generate channel matrix \mathbf{H} using (2).

for $q = 1$ to $|\mathbf{Q}|$ **do**

3. Calculate $\mathbf{H}' = \mathbf{H}_T^q$ which is channel matrix over antenna selection possibility q .

for $k = 1$ to K **do**

4. Calculate $\gamma_k^{(q,i)}$ using (7) with proper \mathbf{F} given by (6) and \mathbf{H}' .

end

5. Calculate the sum-rate using (8) and $\gamma_k^{(q,i)}$ s.

end

6. Labeling: find $\mathcal{D}_{k,i} = \operatorname{argmax}_q \sum_{k=1}^K \log(1 + \gamma_k^{(q,i)}) \forall q$.

end

7. Concatenation: concatenate training data and corresponding labels as $\mathcal{T} = \{\mathbf{H}^{(i)} | \mathcal{D}^{(i)}\}$, $\forall i \in \mathbb{I}$.

TABLE I
CNN ARCHITECTURE PARAMETERS IN DETAIL.

| Layers | Activations | Learnables |
|--|--------------------------|---|
| Input | $128 \times 4 \times 3$ | - |
| Conv. 2D $256 \times [32 \times 2 \times 3]$ | $97 \times 3 \times 256$ | weights : 3×2^{14} bias : 256 |
| Batch norm. 256 channels | $97 \times 3 \times 256$ | offset : 256 scale : 256 |
| Max pooling | $72 \times 3 \times 256$ | - |
| ReLU | $72 \times 3 \times 256$ | - |
| Conv. 2D $32 \times [32 \times 2 \times 256]$ | $41 \times 2 \times 32$ | weights : 2^{19} bias : 32 |
| Batch norm. 32 channels | $41 \times 2 \times 32$ | offset : 32 scale : 32 |
| Max pooling | $16 \times 2 \times 32$ | - |
| ReLU | $16 \times 2 \times 32$ | - |
| Fully connected 1024 | 1024 | weights : 2^{20} bias : 2^{10} |
| ReLU | 1024 | - |
| Fully connected 64 | 64 | weights : 2^{16} bias : 64 |
| ReLU | 64 | - |
| Fully connected 16 | 16 | weights : 1024 bias : 16 |
| ReLU | 16 | - |
| Flatten \mathbb{C} | \mathbb{C} | weights : $\mathbb{C} \times 16$ bias : \mathbb{C} |
| Softmax | \mathbb{C} | - |

V. SIMULATION RESULTS AND DISCUSSION

In this section, the simulation process is described. We also address the challenges during the development of PaSUM-CNN and the provided solutions.

Table I summarizes the layer parameters of each CNN unit depicted in Fig. 3. We use mini-batches of size 250 in the training process with a learning rate of 4×10^{-4} .

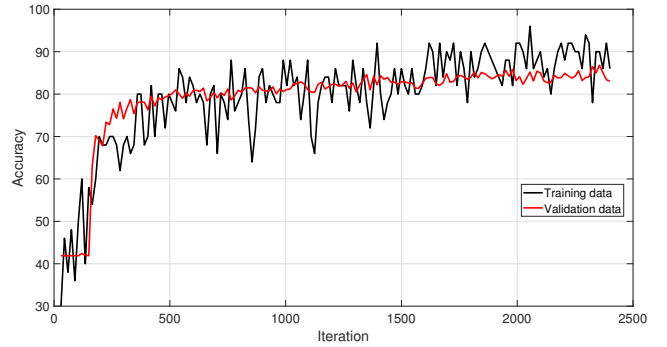


Fig. 4. Convergence of the training phase of the PaSUMCNN method.

Our designed network has two Convolutional blocks including a set of CL-BN-MP-AF in the input. Adding more blocks had no effect on improving the performance of the system with the same amount of training data. All the simulation parameter values are mentioned in Table II.

A. Managing the over-fitting problem

Usually, we divide our labeled data into two parts: a major part for training the network and a minor part to validate the accuracy of the trained network. We used 20% of the labeled samples for the validation part. One of the common issues that happens during the process of training a machine is the *over-fitting* problem, when the networks adapts itself more to the variability of the training data and it fails to act properly with a new data set. We use three methods to deal with this issue [6]:

- **Normalizing data:** We use BN layers and also (10) to avoid any bias in the input data.
- **Dropout layer:** These layers randomly discard some of the neurons of FC layers according to a probability p at each epoch of the training. This helps in dropping the neurons with dominant weights in the network allowing the prediction of new data sets.
- **Regularization factor:** Adding a penalty term to the loss function of the network assists in bypassing the over-fitting. We use a first order penalty term in our network with regularization factor ϵ .

Using these methods, the convergence behaviour of accuracy in the training phase of the network is presented in Fig. 4 for both of the training and validation data. Both curves reach 80% accuracy levels at early stages of the training (1/5th of the training period). Thus, we can compromise a bit on the accuracy of the model to have a faster training phase for delay sensitive applications.

B. Numerical Results

Once the network is trained, we use it to perform SUM on newly generated channel matrices. The results are shown in Fig. 5, which compares the sum-rate of the optimal SUM

TABLE II
SIMULATIONS PARAMETERS IN DETAIL.

| Variable | Value | Variable | Value |
|--------------|--------------|-----------------|-------------|
| M | 256 | K | 9 |
| \mathbb{C} | 12 | N_{max} | 40 |
| \mathbf{P} | \mathbf{I} | \mathbf{I} | 5000 |
| β | 2 | α | 3 |
| λ | 2.6GHz | Antenna spacing | $\lambda/2$ |
| (l_1, l_2) | (50, 100) | ζ | $M/4$ |
| p | 0.6 | ϵ | 0.0015 |

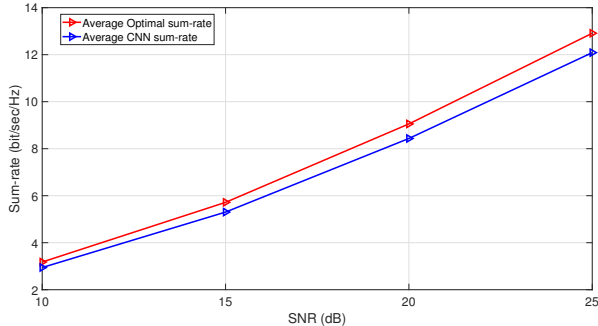


Fig. 5. Sum-rate of the optimal and learning-based solutions.

(exhaustive search) and PaSUMCNN versus different pre-processing SNR values. As it can be seen the performance gap is very small and ranges between 6.4% to 7.4%. Moreover, our assumption on having consecutive antenna sets for the SUM solution space is not creating a huge difference here and we can claim that it is a valid simplifying assumption. This proves the near-optimal output of the PaSUMCNN in the XL-MIMO systems.

C. Implementation aspects

In this subsection we roughly compare the computational complexity of the PaSUMCNN and the exhaustive search method. For the PaSUMCNN method as demonstrated in Table I, the dominant number of weights is 2^{20} which controls the complexity of the multiplications for this method. It also has K parallel units that each have the same complexity which roughly gives $K \times 2^{20}$ computations per SUM and it is independent of the number of the classes \mathbb{C} . On the other hand, in exhaustive search we look into $K^{\mathbb{C}}$ possibilities and for each of them the matrix inversion of ZF needs K^3 operation giving roughly $K^{\mathbb{C}+3}$ computations per AS. As an example and with our simulation parameters, the complexity gain of PaSUMCNN is approximately $\frac{K^{\mathbb{C}+3}}{K \times 2^{20}} = 2 \times 10^7$. It is worth mentioning that this complexity gain of the PaSUMCNN creates a great opportunity to implement this method for practical applications. Training of the network occurs offline, then at each time we only need to feed the CSI and execute a series of matrix multiplications within each of the networks.

VI. CONCLUSIONS

In this work, we have presented a deep learning based solution to optimize the operation of XL-MIMO arrays. In particular, our solution seeks an optimal mapping of users to

parts of the array, such that the DL sum-rate using a truncated ZF precoder is maximized. Our results show that a properly trained network is able to solve this problem nearly as well as an optimal mapping algorithm, while proposing a competitive solution with respect to the current state-of-the-art solutions that only consider small sized systems.

The results presented in this work lead us to two general conclusions: 1) increasing the size of current massive MIMO arrays is one of the most promising avenues to continue boosting the spectral efficiency of current and future wireless systems, and 2) the recent developments in automated learning algorithms, such as deep learning, enable a new research direction in the communication systems to model and solve complex problems. We conjecture that the combination of these two aspects will be one of the leading trends in the developments of wireless communications in the future years.

REFERENCES

- [1] F. Boccardi, R. W. Heath, A. Lozano, T. L. Marzetta, and P. Popovski, "Five disruptive technology directions for 5g," *IEEE Communications Magazine*, vol. 52, no. 2, pp. 74–80, February 2014.
- [2] E. Björnson, L. Sanguinetti, H. Wymeersch, J. Hoydis, and T. Marzetta, "Massive mimo is a reality-what is next? five promising research directions for antenna arrays," *arXiv preprint arXiv:1902.07678*, 2019.
- [3] E. De Carvalho, A. Ali, A. Amiri, M. Angelichinoski, and R. W. Heath Jr, "Non-stationarities in extra-large scale massive mimo," *arXiv preprint arXiv:1903.03085*, 2019.
- [4] S. Hu, F. Rusek, and O. Edfors, "Beyond massive mimo: The potential of positioning with large intelligent surfaces," *IEEE Transactions on Signal Processing*, vol. 66, no. 7, pp. 1761–1774, April 2018.
- [5] A. Amiri, C. N. Manch'on, and E. de Carvalho, "A message passing based receiver for extra-large scale mimo," *arXiv preprint arXiv:1912.04131*, 2019.
- [6] C. M. Bishop, *Pattern Recognition and Machine Learning (Information Science and Statistics)*. Berlin, Heidelberg: Springer-Verlag, 2006.
- [7] I. Goodfellow, Y. Bengio, and A. Courville, *Deep Learning*. MIT Press, 2016.
- [8] T. O'Shea and J. Hoydis, "An introduction to deep learning for the physical layer," *IEEE Transactions on Cognitive Communications and Networking*, vol. 3, no. 4, pp. 563–575, Dec 2017.
- [9] A. Ali, E. de Carvalho, and R. W. Heath, "Linear receivers in non-stationary massive mimo channels with visibility regions," *IEEE Wireless Communications Letters*, 2019.
- [10] W. Xia, G. Zheng, Y. Zhu, J. Zhang, J. Wang, and A. P. Petropulu, "A deep learning framework for optimization of miso downlink beamforming," *arXiv preprint arXiv:1901.00354*, 2019.
- [11] J. Joung, "Machine learning-based antenna selection in wireless communications," *IEEE Communications Letters*, vol. 20, no. 11, pp. 2241–2244, Nov 2016.
- [12] A. M. Elbir, K. V. Mishra, and Y. C. Eldar, "Cognitive radar antenna selection via deep learning," *IET Radar, Sonar & Navigation*, 2019.
- [13] Y. Gao and T. Kaiser, "Antenna selection in massive mimo systems: Full-array selection or subarray selection?" in *IEEE Sensor Array and Multichannel Signal Processing Workshop (SAM)*, July 2016, pp. 1–5.
- [14] H. Q. Ngo, E. G. Larsson, and T. L. Marzetta, "Energy and spectral efficiency of very large multiuser mimo systems," *IEEE Transactions on Communications*, vol. 61, no. 4, pp. 1436–1449, April 2013.
- [15] D. Tse and P. Viswanath, *Fundamentals of Wireless Communication*. New York, NY, USA: Cambridge University Press, 2005.
- [16] A. Adhikary, J. Nam, J. Ahn, and G. Caire, "Joint spatial division and multiplexing the large-scale array regime," *IEEE Transactions on Information Theory*, vol. 59, no. 10, pp. 6441–6463, Oct 2013.
- [17] A. Amiri, M. Angelichinoski, E. de Carvalho, and R. W. Heath, "Extremely large aperture massive mimo: Low complexity receiver architectures," in *2018 IEEE Globecom Workshops (GC Wkshps)*, Dec 2018, pp. 1–6.